The 7th Indonesia Japan Joint Scientific Symposium (IJJSS 2016)
Chiba, 20-24 November 2016

DEVELOPMENT L-BAND ANTENA WITH LOW POWER FOR CIRCULARLY POLARIZED-SYNTHETIC APERTURE RADAR (CP-SAR) APPLICATION ON UNMANNED AERIAL VEHICLE (UAV)

Muhammad Fauzan Edy Purnomo[a,b], Rahmadwati[c], Hadi Suyono[d], Rudy Yuwono[e], Joshapat Tetuko Sri Sumantyo[f]

[a,c,,d,e]*Electrical Engineering Department, Faculty of Engineering, Brawijaya University, Malang 65145, Indonesia*
[b]*Electrical Engineering and Computer Science, Kanazawa University, Kakuma-machi, Kanazawa, Ishikawa 920-1192, Japan*
[f]*Center for Environmental Remote Sensing (CEReS), Josaphat Microwave Remote Sensing Laboratory (JMRSL), Chiba University, Chiba 263-8522, Japan*

Abstract

The development of radar technology, Synthetic Aperture Radar (SAR) and Unmanned Aerial Vehicle (UAV) relatively fast and demanding needs of communication facilities and infrastructure that has a variety of platforms and imaging of high quality, which can generate data processed with high resolution and a better image for all types of terrain explored. In this paper, it obtain the array construction antenna for Circularly Polarized-Synthetic Aperture Radar (CP-SAR) embedded an UAV with compact, small, and simple configuration i.e. the developing a single and 16-element array antenna with simple equilateral triangular-shaped, tip-truncated patch for CP-SAR operated in the L-band.

An equilateral triangular truncated microstrip antenna is proposed for circularly-polarized synthetic aperture radar (CP-SAR) systems operated in L-Band (1.27 GHz). Electromagnetically coupled, dual-feeding method is applied to generate the circularly polarized wave radiating from the patch. The performance characteristics of these antennas are circular polarization, both circular to the left or to the right, making them easier to capture images of objects on earth for processing information content that can be utilized. The feeding design concept is implemented by simple feed with likely length square-shape that can generates two modes using perturbation segment (*as*) and stimulate the same current distribution at each patch and also excite both a left-hand circular polarization (LHCP) and a right-hand circular polarization (RHCP). The simulated antenna based on the IE3D software using moment method gives a good circular polarization at the center frequency of 1.27 GHz with an impedance bandwidth of 0.5% and 3-dB axial ratio bandwidth of 100%, satisfying the specification for our circularly polarized synthetic aperture radar intended for using on-board an UAV.

Keywords

Single and 16-element; Equilateral triangular-shaped; Tip-truncated; Simple feed; Circularly polarized

1. Introduction

Synthetic aperture radar (SAR) in the microwave band is active sensors which can produce high-resolution images in the microwave band. The use of microwave frequencies allows penetration through the clouds, and even through the forest canopy for bands of lower frequencies. Conventional SAR systems have been based on a linear polarized (LP) antenna system. A circularly polarized SAR (CP-SAR) which will be launched on-board micro-satellites currently developed in Microwave Remote Sensing Laboratory (MRSL) from the Center for Environmental Remote Sensing (CeRES), Chiba University (Sri SU et al, 2009). As part of this project, the development of CP-SAR air is also conducted to gain enough knowledge about CP-SAR sensor system. L-band CP-SAR system will be designed for operation on-board the unmanned aerial vehicle (UAV). However, there are limitations due to the phenomenon of propagation such as variation within geometrically between the radar system and the Earth, the phase shift when the microwave attack smooth, reflective surfaces, etc. this phenomenon causes the modulation unwanted signal backscatter, redistribution random back signal-energy and in the end, the image formed will face blurring and defocusing spatial variants and unambiguous identification low backscatter different features in a scene (Yohandri et al, 2011). Especially for the propagation space, electromagnetic waves propagate through the ionosphere interact with electrons and magnetic fields.

The full characterization of SAR signals backscattered from random objects can only be made possible through the use of circular polarization. Therefore, compared with the linear SAR sensor, a large amount of information about the scene and the target is imaged will be provided with a CP-SAR sensor (Baharuddin et al, 2009). The results of synthesis of circularly-polarized data are far better compared to those constructed from the conventional linearly-polarized data. In addition, more sensitive measurements may be obtained by using circular polarization when the surface roughness was studied using polarimetric SAR data (Mattia, 1997). This work focuses on the design CPSAR L-band antenna both single element and 16-element array with a new shape i.e. equilateral triangular truncated antenna using proximity fed.

The purpose of the present paper is to describe the development of the LHCP and RHCP single and 16-element array microstrip antenna installed on UAV. In general, a microstrip antenna can attain a narrow frequency bandwidth at the expense of a low gain. As compared with conventional microwave antennas, a microstrip antenna has additional advantages such as a compact size, light weight, conformability to surfaces of substrates, low cost, and easier integration with other circuits and versatility (Garg et al, 2001). For CP-SAR applications, an array configuration must be adopted to satisfy the requirement of the system. Here, we propose an L-band CP-SAR antenna consisting of single and 16-element of simple equilateral triangular truncated microstrip antenna with 1 and 16 feeding.

2. Configuration of Array Antenna

The antenna structure of single element (Basari et al, 2006) and sixteenth-element array antenna which carried out the design and modeling are depicted in Figure 1. and Figure 2., respectively. Design and modeling software refers to the antenna IE3D to get the antenna receiving and transmitting placed in the fuselage UAV with working frequency of 1.27 GHz. More complete data for the technical specifications of CP-SAR antenna on a UAV can be seen in Table. 1. The shape of the antenna to be made is the truncated form of an equilateral triangle, made of type NPC (Nippon Pillar Packing)-H220A (Edy PUR and Sri SU, 2011), with a relative permittivity of 2.17, loss tangent of

0.0005, and the substrate thickness of 1.6 mm x 2 (patch radiating and feeding) = 3.2 mm.

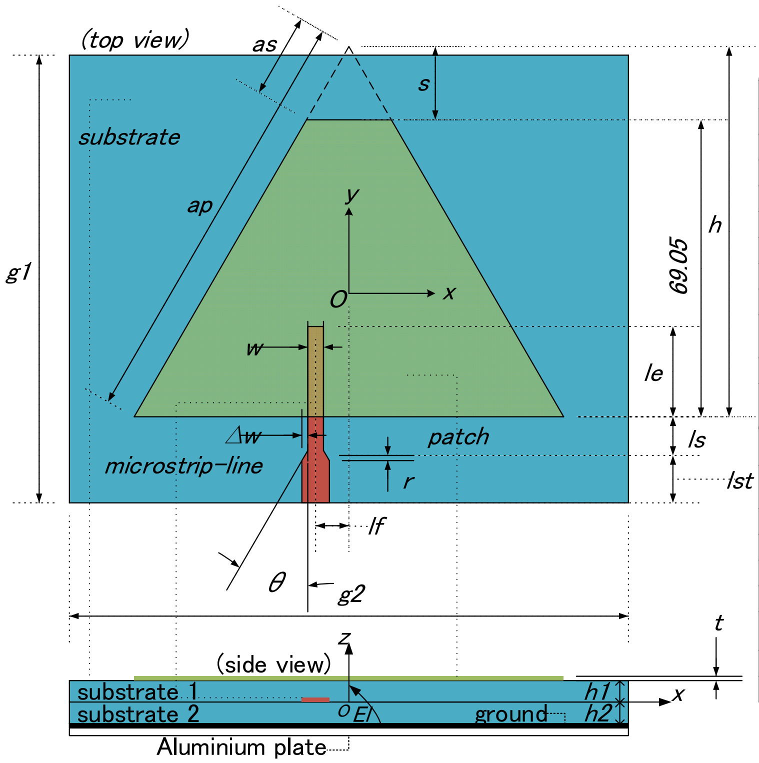

Legend		
Antenna: CP-SAR 1 elemen		
Parameters	Symbols	Dimensions
patch length	ap	99,37 mm
length_tip	as	19,64 mm
ground height	g1	104,05 mm
ground length	g2	129,38 mm
patch height	h	86,06 mm
substrate 1 height	h1	1,6 mm
substrate 2 height	h2	1,6 mm
feed length from edge of microstrip	le	21,00 mm
feeding shift	lf	7,68 mm
feed length from connector	ls	8,99 mm
microstrip-line length	lst	11,01 mm
connecting length between ls & lst	r	1,175 mm
height_tip	s	17,01 mm
thickness copper	t	0,035 mm
stripline width	w	3,64 mm
Δw	Δw	1,36 mm
angle between ls & lst	θ	30,06°
relative permittivity	ε	2,17
loss tangent	δ	0,0005

Figure 1. the construction of single element antenna

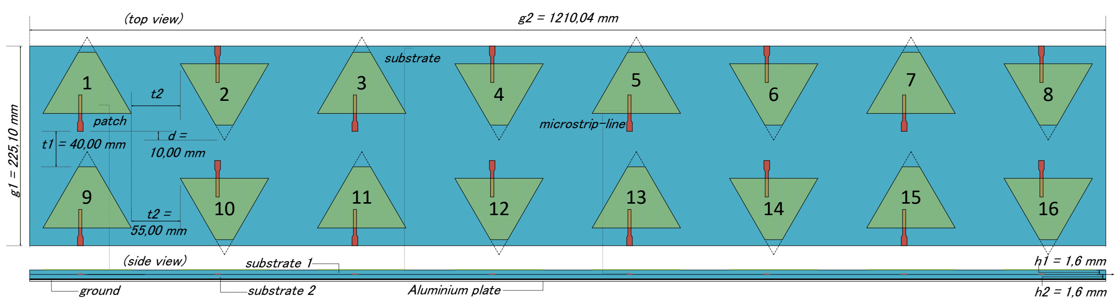

Figure 2. the construction of 16-elements array antenna

While, the truncated function is to make circular polarization both LHCP and RHCP depend on the loci of feeding antenna. Similar with the truncated function, for more stability of it, the proximity technic of fed operated for making smooth circular polarized, to wide bandwidth, increase the gain and also to adjust coupling with the element beside it (Edy PUR et al, 2015). In matter of coupling, the distance between apex of array elements both of beside of it and upper or below of it are set 55 mm and 40 mm, respectively. It is meant to reduce isolation with each closer patch and thus to get sufficient gain for obtaining the minimum requirement 3 dBic for single element. Usually, for decreasing coupling to patch element closer each other, need the distance between the patch element (in this case 1/3 *h*, where *h* is a height of patch antenna) to the other closer patch element (*t1*= 47.01 mm and *t2* = 55 mm) is based on the formula 0.5 λ < *d*

<λ, where λ is wavelength of used (Tanaka et al, 2006). Moreover, the size of ground $g1$ = 233.11 mm and $g2$ = 1209.96 mm

Table 1. Technical specification of CP-SAR antenna on-board UAV

No	Antenna Parameters	Specification for UAV
1.	Resonance Frequency (Center) (GHz)	1,27
2.	Pulse Band Wide (MHz)	233,31
3.	Axial Ratio (dB)	≤ 3
4.	Antenna Efficiency (dBic)	>80 %
5.	Gain Antenna (degree)	14,32
6.	Azimuth Beamwidth (degree)	≥ 6,77^0
7.	Elevation Beamwidth (degree)	3,57^0 – 31,02^0
8.	Antenna Size (m)	1,5 x 0,4
9.	Polarization (Tx/Rx)	RHCP + LHCP

3. Results

3.1 Single Antenna

In Figure 3. to Figure 5., the images show the simulation results of antenna gain of LHCP, RHCP and the total gain of a single antenna with a truncated equilateral triangle proximity fed. Gain total shows the stability of the gain because of an accumulation of LHCP and RHCP gain with a value of 4 dBi which is relatively better than the LHCP and RHCP gain at target frequency of 1.27 GHz. A single antenna with a reduction in length-patch (truncated) makes the total vector current distribution is reduced in the truncated area which caused wide-band antenna becomes narrow (Edy PUR et al, 2016).

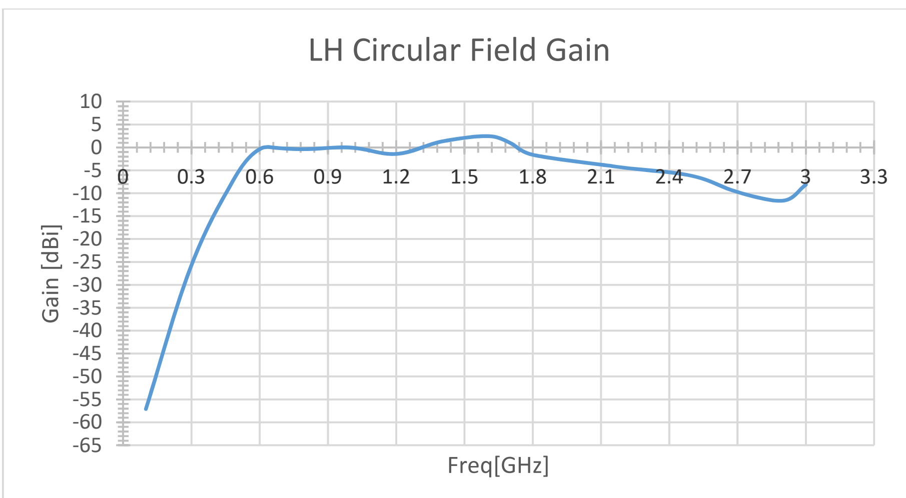

Figure 3. LHCP gain

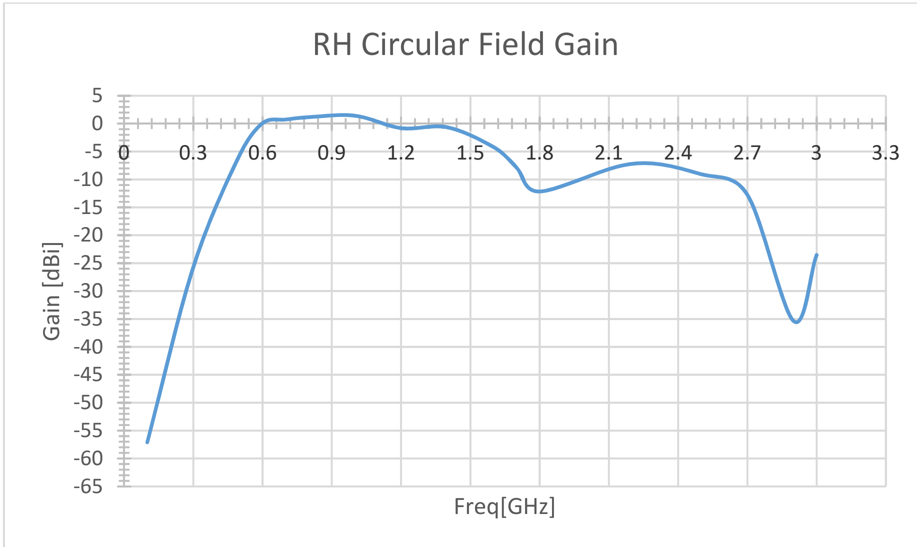

Figure 4. RHCP gain

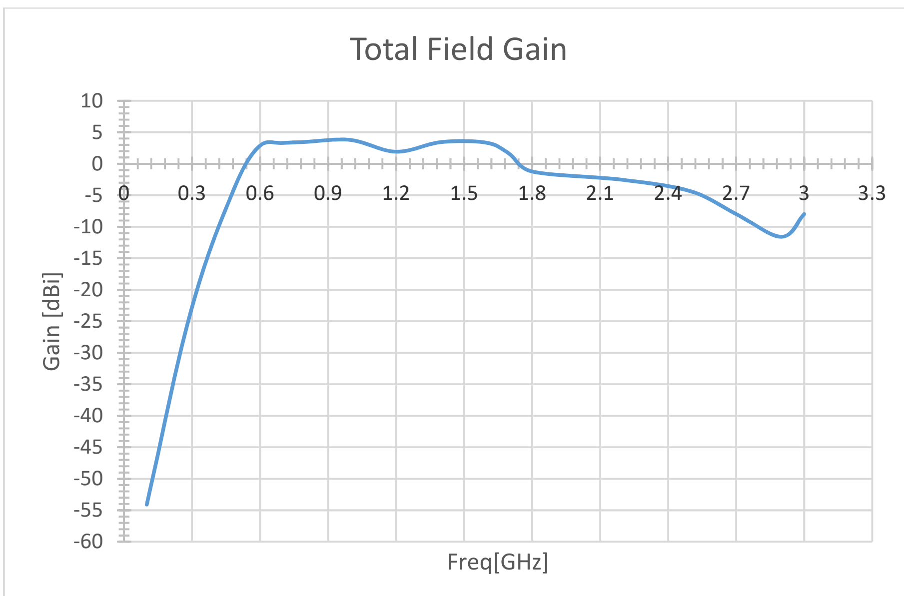

Figure 5. total gain

Figure 6. shows the value of axial ratio (*Ar*) for simulation at the target frequency of 1.27 GHz at 0.0001 dB. In addition, *Ar*-3dB bandwidth of the antenna closer to the maximum of 100%.

Figure 7. shows the relationship between the *S*-parameters and frequencies for simulation of antenna *Tx*/*Rx*. In this figure, it can be seen that the *S*-parameters of an equilateral triangle truncated antenna at the target frequency of 1.27 GHz approximately -12.3 dB.

In the Figure 8. describes the characteristics of the input impedance of the *Tx*/*Rx*. This figure shows that the real part of the simulation has the result of close to 50 Ω. While the reactance of the equilateral triangle truncated antenna also close to 0 Ω. Furthermore, the impedance bandwidth (below -10 dB) of the antenna is about 2 MHz.

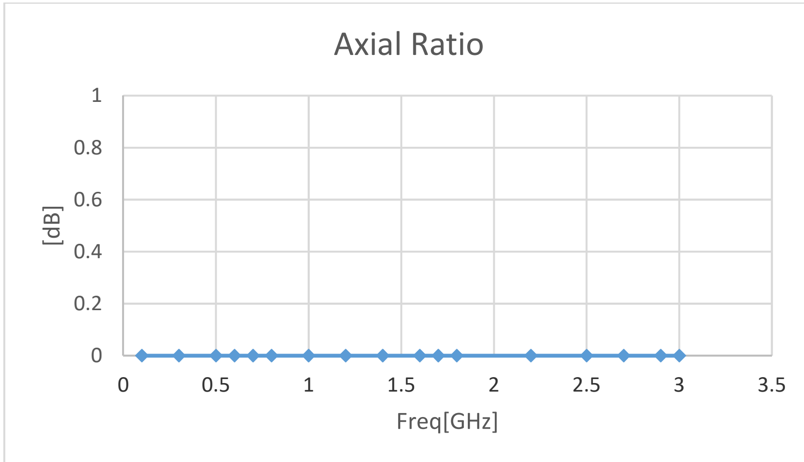

Figure 6. axial ratio

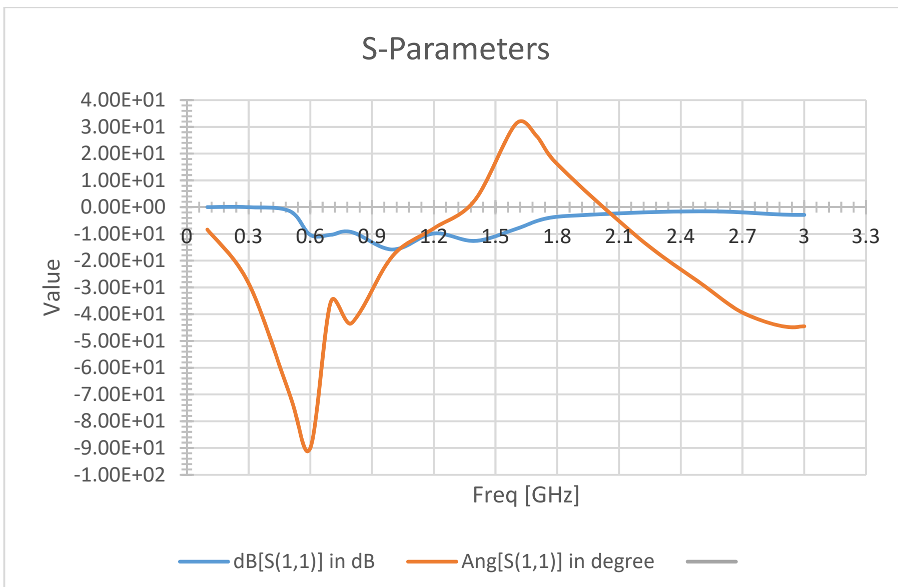

Figure 7.*s*-parameter

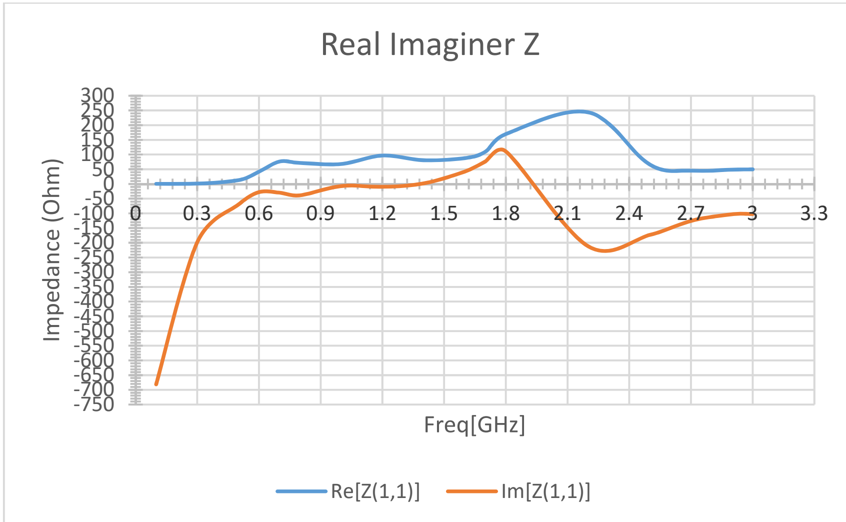

Figure 8.input impedance

Figure 9. and Figure 10. show the efficiency of the antenna and the radiation efficiency in which the radiation efficiency (60%) greater than the antenna efficiency (55%) on a target frequency of 1.27 GHz. This is due to the radiation efficiency parameter depends only on the values of loss while on the efficiency of antenna radiation other than radiation loss is also a loss of materials, dielectric loss and others.

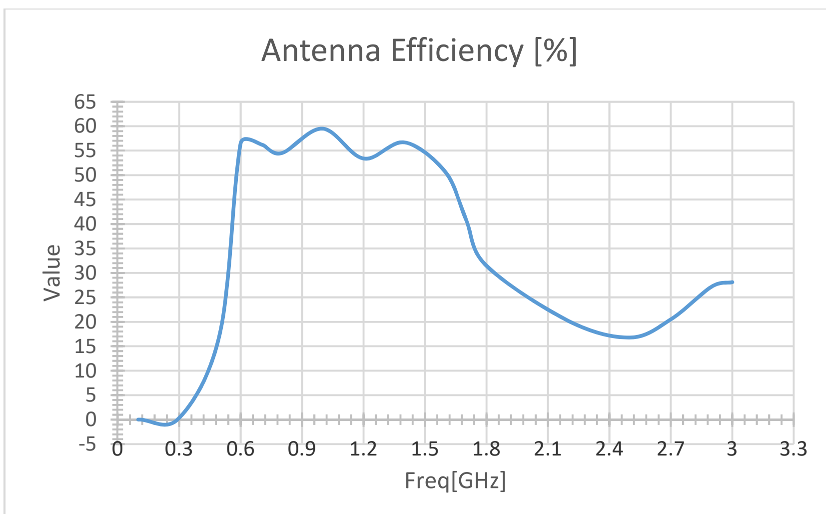

Fig.ure 9. antenna efficiency

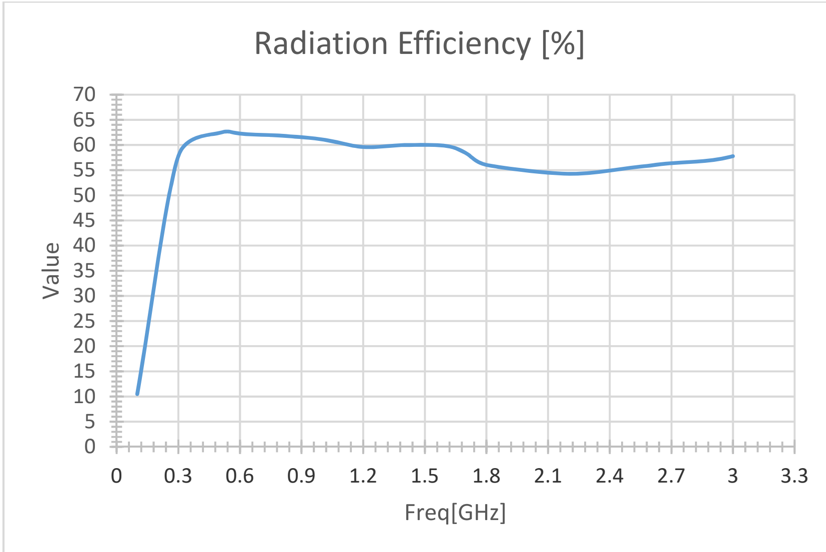

Fig.ure 10. radiation efficiency

3.2 Array Antenna

In Figure 11 until Figure 13, the images show the simulation results gain antenna among LHCP, RHCP and the total gain of the 16-element array equilateral triangular truncated antenna which used the proximity fed. Gain total shows the stability in value due to an accumulation of LHCP and RHCP gain accumulation with a value of 12.5 dBi. While the LHCP gain is relative the same with RHCP gain at the target frequency 1.27 GHz about 9.4 dBi. The 16-element rray antenna are made by combining several single patch to increase the gain as long as the coupling that occur in each single element is to set a minimum distance between the closed element about ¼ wavelength.

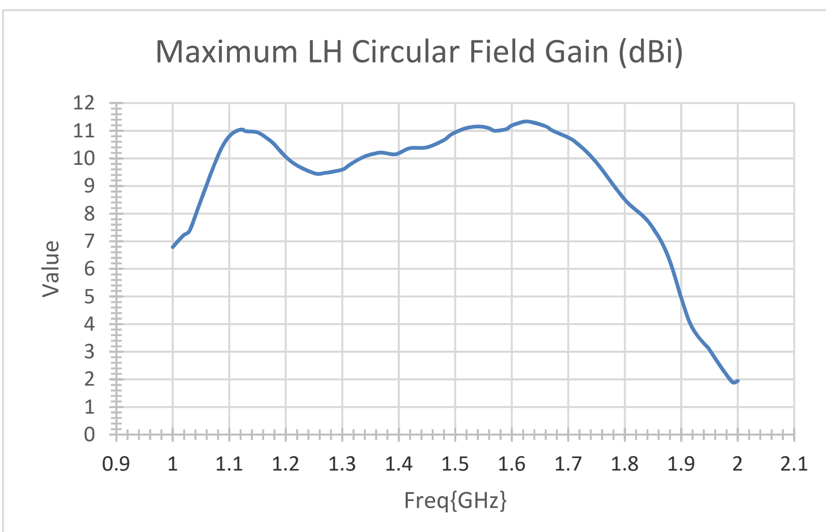

Fig.ure 11. LHCP gain

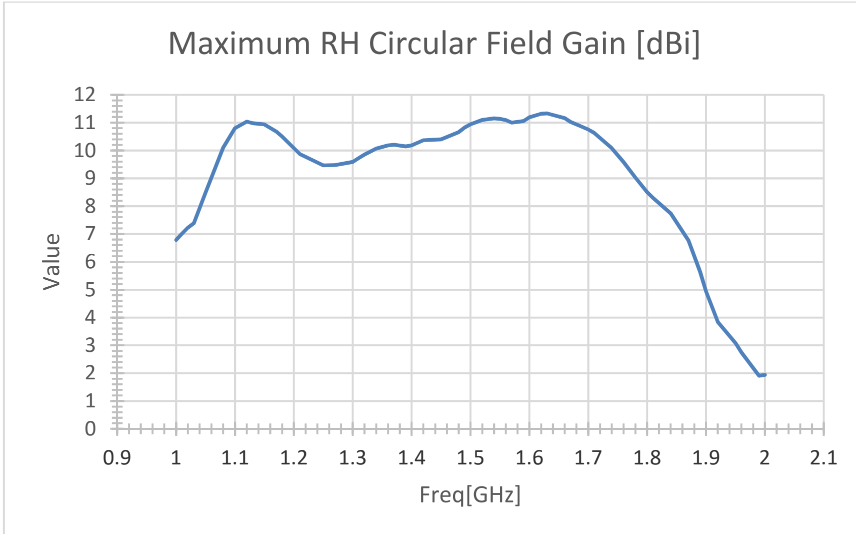

Fig.ure 12. RHCP gain

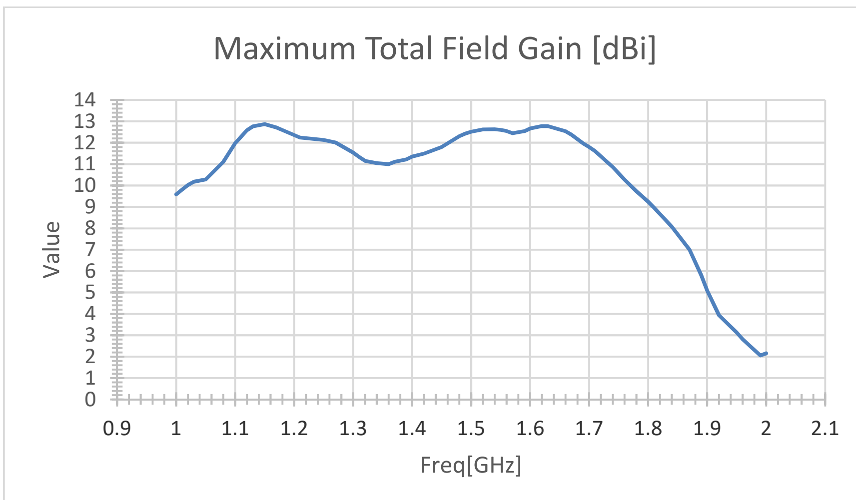

Fig.ure 13. total gain

Figure 14. shows the value of axial ratio (*Ar*) 16-element array antenna that is relatively the same the result of a single antenna for simulation at the target frequency of 1.27 GHz amounted to 0.0001 dB. In addition, *Ar*-3dB bandwidth of the antenna approach maximum of 100%.

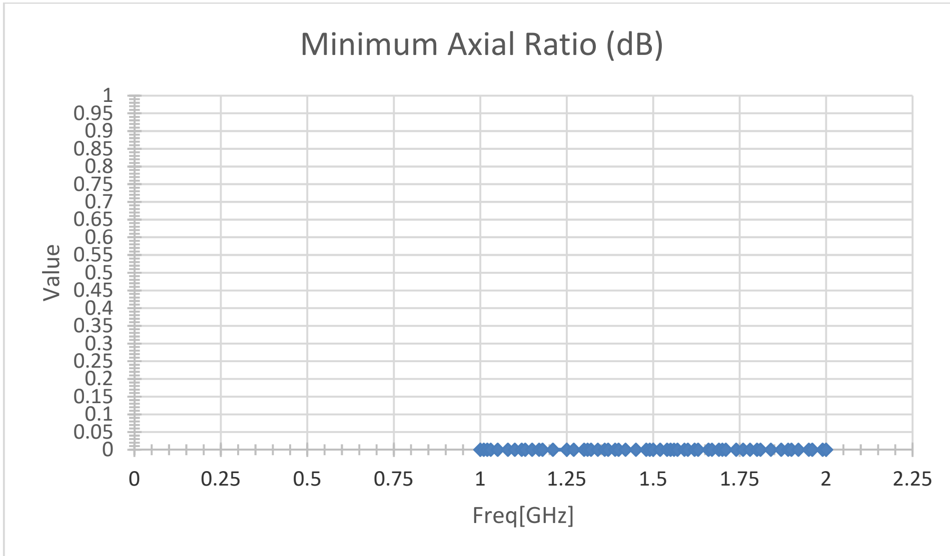

Fig.ure 14. axial ratio

Figure 15 until Figure 18, the figures show the relationship among the *S*-parameters and frequencies for element *S*-11 (represented by the elements patch number 5), *S*-12, *S*-19, *S*-910 from the simulated antenna Tx / Rx. On figure, it is seen that the *S*-12 and *S*-910 has a relatively similar results for patch elements are located adjacent positions (left-right), but very different from the *S*-19 because of the position of the patch antenna is top-down. It can be seen that the effect of coupling loss of each patch antenna occurs that the *S*-19 is relatively better than the *S*-12 and *S*-910, each value in the target frequency range of 1.27 GHz about -21.7 dB and -19.5 dB, respectively. While the value of the *S*-11 is decreased comparing with the single element antenna (-12.3 dB) of approximately -6.7 dB at the target frequency 1.27 GHz. This matter due to the 16-elements array antenna fed using 16 feeding and all of each element are not still matched yet. Hence, it is very important in order to obtain loss minimum possible value and to distribute the flow maximum power and optimum gain, the optimized array antenna design is necessity.

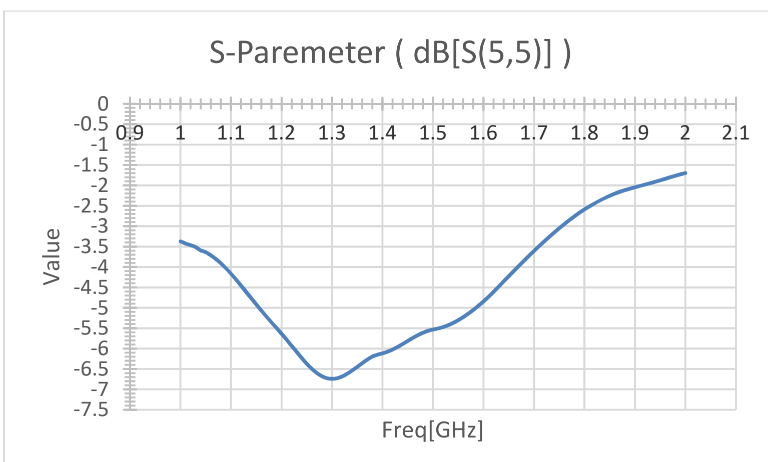

Fig.ure 15. S-11

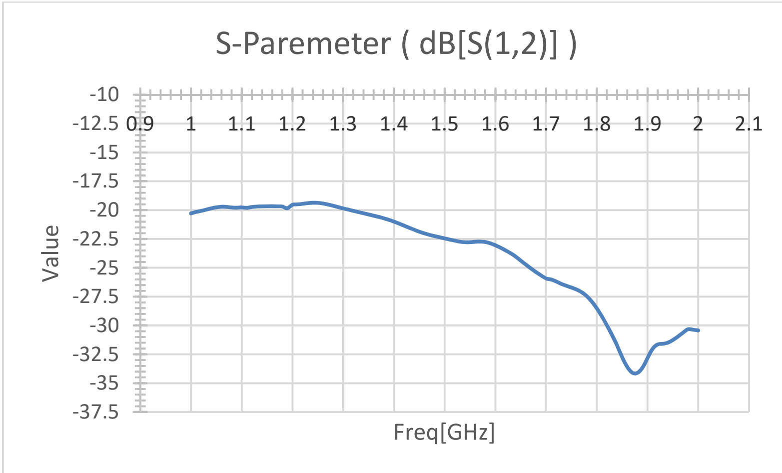

Fig.ure 16. S-12

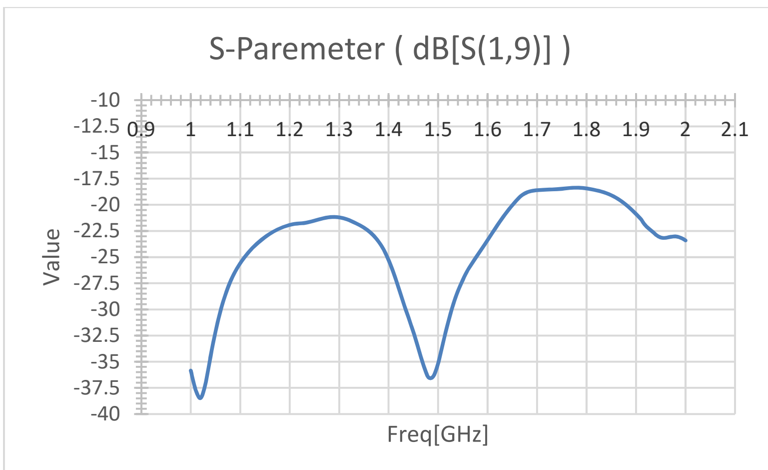

Fig.ure 17. S-19

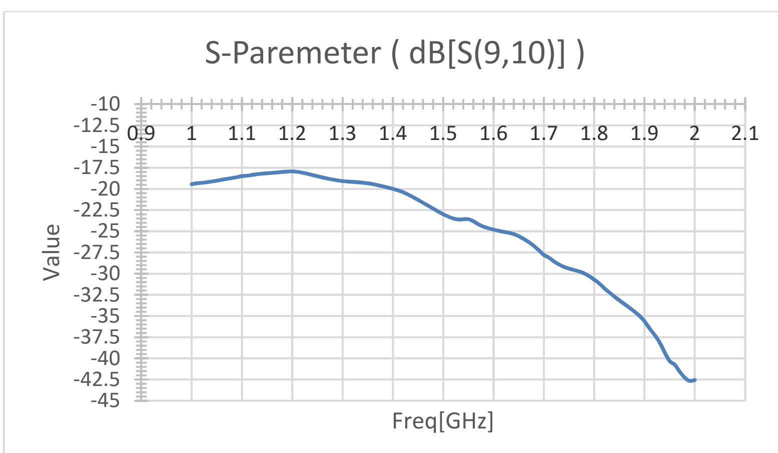

Fig.ure 18. S-910

4. Conclusion

The research process has already discussed to the stage of the single antenna design and array antenna 16-elements of the equilateral triangle truncated with proximity fed, where its performances still need to be optimized especially value the gain and efficiency of the antenna. For the value of *S*-parameter of single antenna is good enough because it was below -10 dB, however for the array antenna still need to be optimized because it was still in the upper of -10 dB. While the value of input impedance for the riel and the imaginer, especially for a single antenna ranges approaching 50 Ω and 0 Ω. The value of the gain of the antenna is increased when compiled 16-elements rather than single element i.e. from the 4 dBi to become 12.5 dBi, while the axial-ratio both single and 16-element array antenna are relatively the same at the target frequency 1.27 GHz approximate 0.0001 dB.

Acknowledgements

The authors would like to thank the Microelectronic Research Laboratory (MeRL), Kanazawa University, Japan for the support and the Center for Environmental Remote Sensing (CEReS), Josaphat Microwave Remote Sensing Laboratory (JMRSL), Chiba University, Japan for joint cooperation in this research and also to thank the Ministry of Research, Technology and Higher Education, Indonesia for supporting research through the research grand on the name of BOPTN 2016.

References

Baharuddin, M., Wissan, V., Sri SUmantyo, J.T. and Kuze, H. (2009). Equilateral Triangular Microstrip Antenna for Circularly-Polarized Synthetic Aperture Radar. Progress in Electromagnetics Research C, Vol. 8, 107–120.

Basari, Sri SUmantyo, J.T., Takahashi, M., Ito, K. (2006). Circularly Polarized Triangular Microstrip Array Antenna Using Single-Fed Proximity-Coupled for Mobile Satellite Communications Applications. Proceeding IJJSS 2006.

Edy PURnomo, M.F. and Sri SUmantyo, J.T. (2011). Design circularly polarized of equilateral triangular hole antenna for SAR (Synthetic Aperture Radar). IEICE Technical Report, ISSN 0913-5685, Vol. 111 No. 239, October 17-19, 2011.

Edy PURnomo, M.F., Pramono, S.H., Pamungkas, M.A. and Taufik. (2015). Study of the effect of air-gap on array microstrip antenna performances for mobile satellite communications. ARPN Journal of Engineering and Applied Sciences ISSN 1819-6608, Vol.10.No.20.

Edy PURnomo, M.F., Suyono, H., Mudjirahardjo, P. and Hasanah R.N. (2016). Analysis performance of singly-fed circularly polarized microstrip antenna for wireless communication. Jurnal TEKNOLOGI e-ISSN 2180-3722, Vol. 78. No. 5-9.

Garg, R., P. Bhartia, I. Bahl, and A. Ittipiboon. (2001). Microstrip Antenna Design Handbook. Artech House, London.

Mattia, F., Toan T.L., Souyris, J., Carolis, G.D., Floury, N., Posa, F. and Pasquariello, G. (1997). The effect of surface roughness on multifrequency polarimetric SAR data. IEEE Trans. Geoscience and Remote Sensing, Vol. 35, No. 4, 954–966.

Sri SUmantyo, J. T., Wakabayashi, H., Iwasaki, A., Takahashi, F., Ohmae, H., Watanabe, H., Tateishi, R., Nishio, F., Baharuddin, M. and Akbar RIZki, P. (2009). Development of circularly polarized synthetic aperture radar on-board microsatellite. PIERS Proceedings, 382–385, Beijing, China, March 23–27, 2009.

Tanaka, T., Houzen, T., Takahashi, M., and Ito, K. (2006). Circularly Polarized Printed Antenna Combining Slots and Patch. IEICE Transaction Communications, VOL.E89—B.

Yohandri, Wissan, V., Firmansyah, I., Akbar RIZki, P., Sri SUmantyo, J.T. and Kuze, H. (2011). Development of circularly polarized array antenna for synthetic aperture radar sensor installed on UAV. Progress In Electromagnetics Research C, Vol. 19, 119-133.